Inorganic Chemistry

Article

Calcium−Phosphonate Interactions: Solution Behavior and Ca²⁺ Binding by 2-Hydroxyethylimino-*bis*(methylenephosphonate) Studied by Multinuclear NMR Spectroscopy

Konstantinos D. Demadis,*,[†] Nikoleta Stavgianoudaki,[†] Gisbert Grossmann,[‡] Margit Gruner,[‡] and Joseph L. Schwartz[§]

Crystal Growth and Design Laboratory, Department of Chemistry, University of Crete, P.O. Box 2208, Voutes Campus, Heraklion GR-71003, Crete, Greece, and Department of Chemistry, Dresden University of Technology, D-01062 Dresden, Germany

The tetra-acid 2-hydroxyethylimino-*bis*(methylenephosphonic acid) (HEIBPH, **1**) and its ring condensation product, the triacid 2-hydroxy-2-oxo-4-phosphonemethyl-1,4,2-oxazaphosphorinane (**2**), were investigated for determination of protonation constants using ^{31}P, ^{1}H, and ^{13}C NMR spectroscopy in a wide pH range. As for other α-amino-phosphonic acids, the first protonation of **1** is straightforward and occurs at the nitrogen, while for **2** the first protonation occurs simultaneously at the exo phosphonate group, allowing estimation of the microscopic protonation constants. The complexation of Ca²⁺ with **1** in a 1:1 molar ratio in aqueous solutions and in the presence of a 5-fold excess Na⁺ is rationalized by the products LCaH₂, LCaH, LCaNaH, LCa, and LCa₂ (L = **1**). Only the phosphonate groups are involved in Ca²⁺ binding at pH > 3, while the phosphonate, hydroxyl, and amine functionalities coordinate to Ca²⁺ at pH > 6−7, as soon as the proton at N is lost. Probable conformation states of ions of **1** and **2** are estimated by means of the dependence of vicinal coupling constants $^{3}J_{HH}$ and $^{3}J_{PC}$ from dihedral angles.

Introduction

Organic phosphonates are used extensively in several important research areas, such as Metal Organic Frameworks (MOFs) and crystal engineering,[1] as well as a number of industrially relevant applications and technologies. Selected applications include chemical additives in water treatment,[2] drug-based regulation of calcium metabolism, or treatment of calcium-related disorders.[3] More specifically, in medical and pharmaceutical applications, phosphonates can regulate calcium phosphate metabolism, particularly in relation to hydroxyapatite, the major mineral constituent of bone.[4] In water treatment programs, they are used as mineral scale inhibitors.[5] The scale inhibition process in industrial process waters is of great economical significance because of the high costs of combating undesirable results of scale forma-tion, the high cost of water in arid areas, and financial losses because of the shutdown of operations.[6] Of the wide variety of phosphonate structures, those possessing the aminomethylenephosphonate group (R₂N−CH₂−PO₃H₂, R = organic moiety) constitute a whole family of phosphonates. Some representative structures are given in Figure 1. We have recently focused on studies with 2-hydroxyethylimino-

* To whom correspondence should be addressed. Tel.: +30-2810-545051. Fax: +30-2810-545001. E-mail: demadis@chemistry.uoc.gr.

† University of Crete.

‡ Dresden University of Technology.

§ Present address: The Nalco Company, Naperville, IL.

(1) (a) Murugavel, R.; Choudhury, A.; Walawalkar, M. G.; Pothiraja, R.; Rao, C. N. R. *Chem. Rev.* **2008**, *108*, 3549. (b) Clearfield, A. *Dalton Trans.* **2008**, 6089. (c) Shi, F. N.; Cunha-Silva, L.; Ferreira, R. A. S.; Mafra, L.; Trindade, T.; Carlos, L. D.; Almeida Paz, F. A.; Rocha, J. *J. Am. Chem. Soc.* **2008**, *130*, 150. (d) Shi, F.-N.; Trindade, T.; Rocha, J.; Almeida Paz, F. A. *Cryst. Growth Des.* **2008**, *8*, 3917. (e) Miller, S. R.; Pearce, G. M.; Wright, P. A.; Bonino, F.; Chavan, S.; Bordiga, S.; Margiolaki, I.; Guillou, N.; Feìrey, G.; Bourrelly, S.; Llewellyn, P. L. *J. Am. Chem. Soc.* **2008**, *130*, 15967. (f) Liang, J.; Shimizu, G. K. H. *Inorg. Chem.* **2007**, *46*, 10449.

(2) (a) Yang, B. *Corrosion* **1995**, *51*, 153. (b) Amjad, Z.; Hooley, J. P. *Tenside., Surfactants, Deterg.* **1994**, *31*, 12. (c) Amjad, Z. *Can. J. Chem.* **1988**, *66*, 2180. (d) Ferguson, R. J. *Industrial Water Treatment* **1993**, *23*. (e) Matty, J. M.; Tomson, M. B. *Appl. Geochem.* **1988**, *3*, 549.

(3) (a) Golomb, G.; Schlossman, A.; Saadeh, H.; Levi, M.; van Gelder, J. M.; Breuer, E. *Pharm. Res.* **1992**, *9*, 143. (b) Golomb, G.; Schlossman, A.; Eitan, Y.; Saadeh, H.; van Gelder, J. M.; Breuer, E. *J. Pharm. Sci.* **1992**, *81*, 1004. (c) Richardson, C. F.; Johnson, M.; Bangash, F. K.; Sharma, V. K.; Sallis, J. D.; Nancollas, G. H. *Mater. Res. Soc. Symp. Proc.* **1990**, *174*, 87. (d) Takeuchi, M.; Sakamoto, S.; Yoshida, M.; Abe, T.; Isomura, Y. *Chem. Pharm. Bull.* **1993**, *41*, 688. (e) Sparidans, R. W.; Twiss, I. M.; Talbot, S. *Pharm. World Sci.* **1998**, *20*, 206.
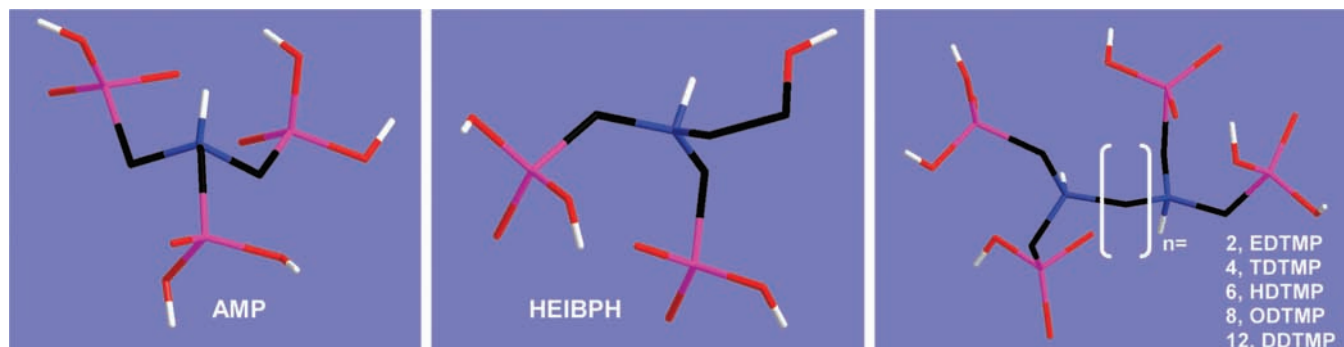
Figure 1. Chemical structures of some aminomethylenephosphonate scale inhibitors in their zwitterionic form. Abbreviations are as follows: **AMP**, amino-*tris*(methylenephosphonate); **HEIBPH**, 2-hydroxyethylimino-*bis*(methylenephosphonate); **EDTMP** ($n = 2$), ethylenediamine-*tetrakis*(methylenephosphonate); **TDTMP** ($n = 4$), tetramethylenediamine-*tetrakis*(methylenephosphonate); **HDTMP** ($n = 6$), hexamethylenediamine-*tetrakis*(methylenephosphonate); **ODTMP** ($n = 8$), octamethylenediamine-*tetrakis*(methylenephosphonate); **DDTMP** ($n = 12$), dodecamethylenediamine-*tetrakis*(methylene-phosphonate). Color codes: C, black; H, white; P, magenta; O, red; N, blue. H's on the methylene groups are omitted for clarity.

bis(methylenephosphonic acid) (HEIBPH, **1**) for several reasons, vide infra. Complex **1** could be envisioned as an analog of AMP (a well-known and commonly used phosphonate[7]), after removing a −CH$_2$PO$_3$H$_2$ arm and replacing it with the −CH$_2$CH$_2$OH ethanolic moiety.

This structural alteration induces profound changes in the behavior of HEIBPH, compared to its close analog, AMP: (a) The number of ionic groups is reduced. (b) HEIBPH is now a *bis*-phosphonate. (c) A weakly coordinating group (−CH$_2$CH$_2$OH) is now present in the molecule. (e) The presence of −CH$_2$CH$_2$OH induces additional "chemistry" on the HEIBPH molecule with the formation of ring **2**, see Scheme 1. (f) The behavior of HEIBPH in solution in the presence of metal ions is profoundly different compared to that of AMP. HEIBPH does not form crystalline one-phase metal−HEIBPH products (under the same conditions of concentration, pH, and temperature as for AMP). In contrast, there has been a large number of metal−AMP structures

Scheme 1
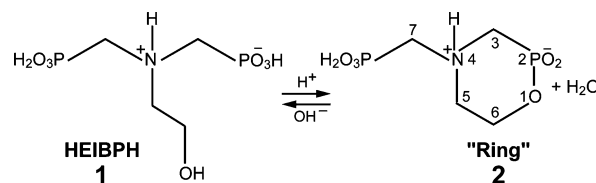
reported in the literature.[8] (g) No metal−HEIBPH compounds have been reported in the literature (with the exception of Na−HEIBPH[9]). The scarcity of structurally characterized metal−HEIBPH compounds may be explained in part by the ring opening/closure in high-/low-pH regions, respectively. It is well-known that the formation of good-quality crystals often depends on ligand purity. In addition, it should be mentioned that syntheses of metal−HEIBPH compounds in high pH regions (the open form is exclusively present) are hampered by the appearance of amorphous solids that are difficult to characterize. Therefore, the above reasons prompted us to initiate a study on the solution behavior of HEIBPH in order to delineate its pH-dependent chemistry, particularly in the presence of biologically and industrially important Ca^{2+} ions.

The method of synthesis of **1** was initially described by Worms and Wollmann[10] and later by others.[11] The "open-form" **1** undergoes a condensation reaction[10] to yield a ring of 2-hydroxy-2-oxo-4-phosphonemethyl-1,4,2-oxazaphos-

(4) (a) Fleisch, H. *Drugs* **1991**, *42*, 919. (b) *The Role of Phosphonates in Living Systems*; Hilderbrand, R. L., Ed.; CRC Press: Boca Raton, FL, 1983. (c) Fleisch, H. *Bone* **1987**, *8*, S23. (d) Rubin, R. P.; Weiss, G. B.; Putney, J. W., Jr. *Calcium in Biological Systems*; Plenum Press: New York, 1985. (e) Schoen, F. J.; Harasaki, H.; Kim, K. M.; Anderson, H. C.; Levy, R. J. *J. Biomed. Mater. Res* **1988**, *22*, 11. (f) Fleisch, H. Bisphosphonates in Bone Disease. *From the Laboratory to the Patient*, 2nd ed.; The Parthenon Publishing Group: New York, 1995.

(5) (a) Zieba, A.; Sethuraman, G.; Perez, F.; Nancollas, G. H.; Cameron, D. *Langmuir* **1996**, *12*, 2853. (b) Amjad, Z. *Langmuir* **1991**, *7*, 600. (c) Kamrath, M. A.; Davis, R. V.; Johnson, D. *Corrosion/94, Paper No. 198*, National Association of Corrosion Engineers: Houston, TX, 1994. (d) Dubin, L. *Corrosion/80, Paper No. 222*, National Association of Corrosion Engineers: Houston, TX, 1980. (e) Black, S. N.; Bromley, L. A.; Cottier, D.; Davey, R. J.; Dobbs, B.; Rout, J. E. *J. Chem. Soc., Faraday Trans.* **1991**, *87*, 3409. (f) Pompe, L. *Z. Anorg. Allg. Chem.* **1983**, *505*, 201–208. (g) Sherren, D. J.; Stone, D.; Brown, P. A.; Watson, M. D. Paper 13, International Water Conference, 1994, p 92. (h) Sweeney, F. M.; Cooper, S. D. Paper SPE 25159, Society of Petroleum Engineers International Symposium on Oilfield Chemistry, New Orleans,LA, March 2−5, 1993.

(6) (a) Oddo, J. E.; Tomson, M. B. *Corrosion/92, Paper No. 34*, National Association of Corrosion Engineers: Houston, TX, 1992. (b) Xiao, J.; Kan, A. T.; Tomson, M. B. *Prepr. Symp. − Am. Chem. Soc., Div. Fuel Chem.* **1998**, *43*, 246. (c) Oddo, J. E.; Tomson, M. B. *SPE Prod. Facil.* **1994**, 47.

(7) (a) Demadis, K. D.; Mavredaki, E. *Env. Chem. Lett.* **2005**, *3*, 127. (b) Bishop, M.; Bott, S. G.; Barron, A. R. *Chem. Mater.* **2003**, *15*, 3074. (c) Vanderpool, D. Paper 40, International Water Conference 1997, p 383. (d) El-Shall, H.; Rashad, M. M.; Abdel-Aal, E. A. *Cryst. Res. Technol.* **2002**, *37*, 1264. (e) Pradip Rai, B.; Rao, T. K.; Krishnamurthy, S.; Vetrivel, R.; Mielczarski, J.; Cases, J. M. *Langmuir* **2002**, *18*, 932.

(8) (a) Daly, J. J.; Wheatley, P. J. *J. Chem. Soc. A* **1967**, 212. (b) Cabeza, A.; Ouyang, X.; Sharma, C. V. K.; Aranda, M. A. G.; Bruque, S.; Clearfield, A. *Inorg. Chem.* **2002**, *41*, 2325. (c) Demadis, K. D.; Katarachia, S. D.; Koutmos, M. *Inorg. Chem. Commun.* **2005**, *8*, 254. (d) Martinez-Tapia, H. S.; Cabeza, A.; Bruque, S.; Pertierra, P.; Garcia-Granda, S.; Aranda, M. A. G. *J. Solid State Chem.* **2000**, *151*, 122. (e) Sharma, C. V. K.; Clearfield, A.; Cabeza, A.; Aranda, M. A. G.; Bruque, S. *J. Am. Chem. Soc.* **2001**, *123*, 2885.

(9) Demadis, K. D.; Baran, P. *J. Solid State Chem.* **2004**, *177*, 4768–4776.

(10) Worms, V. K.-H.; Wollman, K. *Z. Anorg. Allg. Chem.* **1971**, *381*, 260.

(11) (a) Chen, S.-R. T.; Matz, G. F.; Schaper, R. J. (assigned to Calgon Corporation). N,N-bis(phosphonomethyl)-2-amino-1-propanol, derivatives and corresponding lower alkyl ethers and N-oxides thereof for high pH scale control, U.S. Patent 5,259, November 9, 1993. (b) Chen, S.-R. T.; Matz, G. F.; Schaper, R. J. (applicant: Calgon Corporation). N-(2-hydroxyethyl)-N-bis(methylenephosphonic acid) and corresponding N-oxide thereof for high pH scale control. European Patent Application 0 654 248 A, Date of filing: March 30, 1993. (c) Rhodia Company. Patent WO 00/18695. (d) Sun, Y.; Song, J.; Yao, C. *Huagong Shikan* **2002**, *16*, 51–53.

phorinane **2** (Scheme 1) in sufficiently acidic solutions. Hence, we have controlled the conditions of ring formation and performed the preparation of all working solutions from an alkaline stock solution.

The purpose of this study is to use ^{31}P, ^{1}H, and ^{13}C NMR spectroscopy to study the tetra-acid **1** (LH$_4$) and the triacid **2** (RingH$_3$) in solutions in a wide pH range and also to uncover the behavior of **1** in the presence of Ca^{2+} ions. By monitoring the chemical shifts and some coupling constants of the measured nuclei as a function of pH, acid protonation constants and formation constants of calcium complexes were obtained. While X-ray crystallography unequivocally provides the structure of molecules and ions in the solid state, NMR spectroscopy provides insight into the kind of species and their molecular configuration and into some conformation states in solution. It is well-known that the phosphonate groups are involved in calcium binding, but questions exist as to whether the hydroxyl and amine functionalities are involved as well. A combination of these two techniques can be a powerful tool in answering fundamental questions about the behavior of the molecules under study.

Ultimately, it would be useful to utilize these findings to better understand how phosphonates interact with Ca^{2+} ions in solution or with the surfaces of calcium-containing insoluble scale deposits. The ultimate goal of this research approach is to develop organophosphonates *by design* with improved scale inhibition characteristics.[12] The crystal structure of tetrasodium 2-hydroxyethylimino-*bis*(methylenephosphonate) decahydrate was reported recently.[9]

Experimental Section

Materials. A sample of 16.7% HEIBPH (**1**) as an aqueous sodium alkaline stock solution (titration degree[13] $\tau = 5.2$) was obtained from Rhodia Co. (formerly Albright & Wilson), Great Britain. This solution contains some other P-containing acids: 8 mol % H$_3$PO$_3$, 4 mol % hydroxymethanephosphonic acid (conc. solution: $\delta_P = 23.5$ ppm),[14] 2 mol % H$_3$PO$_4$, and 1.5 mol % unknown P acid (see Figure S1, Supporting Information).

Selected samples of 0.11 M HEIBPH were prepared for preliminary single-sample ^{31}P, ^{13}C, and ^{1}H NMR titrations. Detailed studies were performed on 0.050 ($\pm$0.002) M solutions, which were prepared as described below. First, solutions containing 0.10 M HEIBPH of defined titration degrees were prepared by adding specific amounts of 1.00 M HCl or 1.00 M NaOH to 415 μL stock solutions of HEIBPH and then made up to a volume of 3.00 mL with water. Then, two identical volumes of such a solution were diluted (a) with the same volume of water containing 20% D$_2$O and (b) with the same volume of a 0.10 M solution of CaCl$_2$ containing 20% D$_2$O. The accuracy of volume measurement was 5 μL.

Resulting solutions of (a) 0.05 M HEIBPH + 0.26 M Na$^+$ and (b) 0.05 M HEIBPH + 0.05 M CaCl$_2$ + 0.26 M Na$^+$ containing 10 vol % D$_2$O were used for single-sample ^{31}P and ^{1}H NMR titrations. The solutions of series b were measured after standing for several days. For each of the series a and b, about 30 solutions were prepared in a range of titration degrees τ from -10 to $+8$. The samples of series b show some amount of white precipitate in a range of τ from 2.5 to 3.5. The pH of the liquid phase of these samples lies in the range of 5.7$-$8.0, with pH = 6.8 giving a maximum of precipitate containing approximately 30% of the total amount of phosphorus. The results of elemental analysis (C, H, and N) and atomic absorption spectrometry (for Ca^{2+} and Na$^+$) are consistent with the formulation CaNaC$_4$H$_{10}$NP$_2$O$_7$·2H$_2$O (see Table S1, Supporting Information), using the abbreviation LCa-NaH(s) in this paper. A solid-state ^{31}P CP/MAS spectrum of this precipitate shows very broad lines, indicating an amorphous structure. The isotropic chemical shift of 8.0 ppm is an indication of the "betain structure" of this aminomethylenephosphonate (see Table S2, Supporting Information).

Some solutions of 0.05 M HEIBPH were prepared with higher Ca^{2+} concentration. Samples containing 0.1 M CaCl$_2$ at pH > 12.5 give clear solutions, while samples with >0.2 M CaCl$_2$ give at these conditions a precipitate of LCa$_2$(s) without a detectable amount of phosphorus according to NMR measurement of the supernatant liquid. A solid-state ^{31}P CP/MAS spectrum of this precipitate shows also very broad lines. The isotropic chemical shift of 21.4 ppm indicates that the nitrogen is not protonated, as expected. Table S2 (Supporting Information) contains the solid-state data of crystalline LNa$_4$ for comparison, which are similar to the data of solid LCa$_2$.

The ^{31}P and ^{1}H NMR spectra of the most acidic solutions of 0.05 M HEIBPH were measured repeatedly over a period of several months in order to monitor the formation of the ring compound **2**. For the titration of solutions containing ring **2**, the following procedures were used. One part of an HEIBPH stock solution was added to 10 parts of 4 M HCl or to one part of concentrated HCl. Upon standing for two weeks at room temperature, the first solution showed 73% of the ring compound **2** in equilibrium with HEIBPH and was used for measurements of P$-$C-coupling constants. The second solution gave in one week 30% of the ring, 56% HEIBPH, and 14% amino-*tris*-(methylenephosphonate), AMP. Solutions of different pH for the investigation of ring **2** by single-sample ^{31}P and ^{1}H NMR titrations had the composition 0.015 M ring **2** + 0.028 M HEIBPH (**1**) + 0.007 M AMP + 0.26$-$0.34 M Na$^+$ and contained 10 vol % D$_2$O.

Potentiometric Measurements. Measurements of pH were performed with a glass electrode calibrated by standard buffer solutions (pH 4.00, 7.00, and 10.01 from Metrohm Ltd.). We have refrained from calibration of the glass electrode by titration of the strong acid with a strong base (blank titration) to measure hydrogen ion concentration. We have used the following empirical equation, according to Sigel et al.:[15]

$$p[H]_{conc} = pH_{meas} - 0.03 \qquad (1)$$

to convert the measured pH (with a buffer-calibrated glass electrode system) into a concentration p[H]. The p[H]'s of the most acidic and basic solutions were calculated from solution stoichiometry, taking into account the HCl (NaOH) consumption by HEIBPH.[16]

(12) (a) Demadis, K. D.; Sallis, J. D.; Raptis, R. G.; Baran, P. *J. Am. Chem. Soc.* **2001**, *123*, 10129. (b) Demadis, K. D. *Inorg. Chem. Commun.* **2003**, *6*, 527. (c) Demadis, K. D. In *Compact Heat Exchangers and Enhancement Technology for the Process Industries*; Shah, R., Ed.; Begell House Publishers: Redding, CT, 2003, p 483. (d) Demadis, K. D.; Katarachia, S. D. *Phosphorus Sulfur Silicon* **2004**, *179*, 627. (e) Demadis, K. D.; Raptis, R. G.; Baran, P. *Bioinorg. Chem. Appl.* **2005**, *3*, 119–134. (f) Demadis, K. D.; Lykoudis, P. *Bioinorg. Chem. Appl.* **2005**, *3*, 135–149.

(13) The titration degree τ is defined as the molar ratio of univalent base added to a multivalent acid (ligand): $\tau = n_B/n_A$.

(14) Moedritzer, K.; Maier, L.; Groenweghe, L. C. D. *J. Chem. Eng. Data* **1962**, *7*, 307.

(15) Sigel, H.; Zuberbuhler, D.; Yamauchi, O. *Anal. Chim. Acta* **1991**, *255*, 63–72.

(16) Popov, K.; Rönkkömäki, H.; Lajunen, L. H. J. *Pure Appl. Chem.* **2006**, *78*, 663–675.

(17) Davies, C. W. *Ion Association*; Butherworths: London, 1962.

No attempt was made to keep the ionic strength (I) of the single-sample solutions constant, as is usually done in order to make the quotient of activity coefficients into a constant quantity. In fact, the activity coefficients calculated by the Davies equation[17]

$$\log y_i = -A z_i^2 [I^{1/2}/(1 + I^{1/2}) - 0.3I] \quad A = 0.51^{18} \quad (2)$$

are practically invariant over the range of ionic strengths (between 0.25 and 0.6 mol/L) used in this investigation. Specifically, the values of γ_H (the activity coefficient for the hydrogen ion) vary only slightly within a narrow range from 0.73 to 0.74. A second reason for not using additional ionic strength buffers (like NaCl, KCl) is the fact that the desired constant ionic strength would be always disturbed at high titration degrees of multivalent acids due to the formation of highly charged anions.

Solutions containing several weak acids in comparable amounts or as noticeable impurities very often cannot be analyzed by classical potentiometric titrations. In such cases, the NMR-controlled titration allows for simultaneous determination of the equilibrium constants of several acids, if these acids contain NMR-measurable nuclei.

NMR Spectra. All NMR spectra were obtained at room temperature (22 °C) with a 5 mm switchable direct probe on a Bruker DRX 500 spectrometer. The ^{31}P spectra were recorded without ^{1}H decoupling and the ^{1}H spectra without water suppression, using D$_2$O as a lock. The ^{13}C{^{1}H} spectra were locked and referenced to CD$_3$OH ($\delta_C = 49.0$ ppm) and recorded with a resolution of 0.2 Hz/point to determine P$-$C coupling constants. Preliminary investigations had been carried out on Varian UnityI-nova 300 and Bruker AMX 400 spectrometers. These samples were measured without a lock. The ^{1}H chemical shifts were referenced to DSS (0.00 ppm), the ^{13}C shifts also to DSS (-2.58 ppm), and the ^{31}P shifts to aqueous 85% H$_3$PO$_4$ (external 0.0 ppm).

NMR Data Analysis. Determination of cumulative protonation and complex formation constants β of acids **1** and **2** was carried out using the computer program HypNMR2006.[19] Analytical concentrations of investigated weak acids, p[H], and chemical shifts of some nuclei of each solution are required as input. In addition, starting values of all expected equilibrium constants β must be chosen and assigned to the compounds. We have used p$K_w = 13.82$ for all calculations. Because p[H] is a common value for a solution containing several weak acids (byproduct or impurities), the iterative refinement can be done including some weak acids or at least the most important products. In the case of analyzing the titration data of samples containing Ca^{2+}, the iterative refinement of chemical shift versus p[H] does not lead to convergent results. Visual adjustment of δ versus pH curves was satisfactory.

We have obtained ^{31}P chemical shifts and the ^{1}H chemical shifts of CH$_2$ groups from 25$-$30 solutions of different p[H] for one single-sample titration. The total numbers of experimental chemical shifts for each system ranged from 116 to 125. Simulation of titration curves and generation of speciation diagrams were carried out by Hyperquad simulation and speciation program HySS.[20] Detailed information on the HypNMR and HySS programs has been published.[21,22]
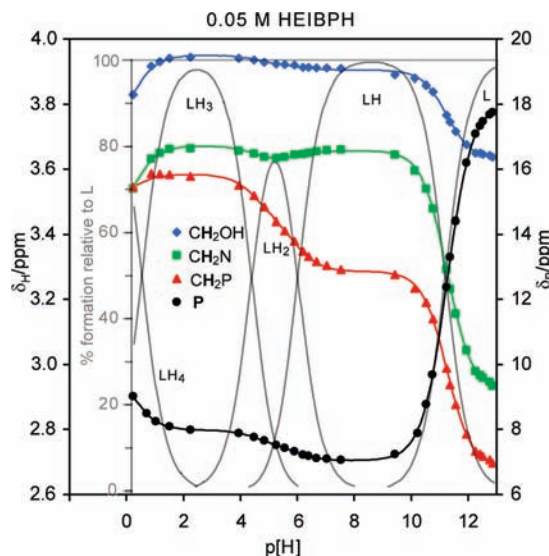
Figure 2. ^{31}P and ^{1}H NMR titration curves δ versus p[H] of 0.05 M HEIBPH (**1**) solutions. The *solid lines* between the experimental values are drawn by joining calculated values, obtained using the refined equilibrium constants and the individual chemical shifts. *Gray lines* show the calculated species distribution of **1** (the charges of species are omitted).

Results and Discussion

All ^{31}P and ^{1}H NMR spectra of freshly prepared titration solutions of HEIBPH (**1**) show the absence of any amount of the condensation product **2** (see Scheme 1). Repeated measurements of ^{31}P and ^{1}H NMR spectra of the most acidic HEIBPH solutions over several months showed that the formation rate of **2** is nearly proportional to the concentration of strong acid (see Figure S2, Supporting Information). After a standing time of 180 days at 22 °C, the formation of nearly 6, 18, and 55% of **2** is obtained for solutions containing 0.05, 0.15, and 0.55 M HCl, respectively.

Acid$-$Base NMR Titration of HEIBPH (1). ^{31}P and ^{1}H titration curves of 0.05 M HEIBPH δ versus p[H][23] are shown in Figure 2. All chemical shift curves show the greatest changes at the range of p[H] 9$-$13 (titration degrees $\tau > 3$)[13] as soon as the last acid proton bound to nitrogen is lost. At $\tau = 3$, the slopes of all titration curves are clearly changed, and the P chemical shift slope even changes sign. The other integer values of τ of the tetra-acid do not exhibit such clear behavior because the protonation constants or the individual chemical shifts of the related species do not differ much.

While the acid/base properties and also the complex formation of substituted imino-*bis*(methylenephosphonic acids) have been investigated,[24−35] to the best of our knowledge, no studies on HEIBPH have been published. The results of our refined calculations by the HypNMR program

(18) Harned, H. S.; Owen, B. B. *The Physical Chemistry of Electrolytic Solutions*, 3rd ed.; Reinhold, New York, 1958.
(19) Gans, P.; Sabatini, A.; Vacca, A. HypNMR 2006, version 3.2.28. http://www.hyperquad.co.uk (accessed Mar 2009).
(20) Gans, P.; Sabatini, A.; Vacca, A. Hyperquad Simulation and Speciation HySS, version 3.2.24, Protonic Software. http://www.hyperquad.co.uk (accessed Mar 2009).
(21) Frassineti, C.; Alderighi, L.; Gans, P.; Sabatini, A.; Vacca, A.; Ghelli, S. *Anal. Bioanal. Chem.* **2003**, *376*, 1041–1052.
(22) Alderighi, L.; Gans, P.; Ienco, A.; Peters, D.; Sabatini, A.; Vacca, A. *Coord. Chem. Rev.* **1999**, *184*, 311–318.
(23) We use in the following the short abbreviation p[H] instead of p[H]$_{conc}$ (see eq 1).
(24) Popov, A.; Rönkkömäki, H.; Popov, K.; Lajunen, L. H. J.; Vendilo, A. *Inorg. Chim. Acta* **2003**, *353*, 1–7.
(25) Motekaitis, R. J.; Martell, A. E. *J. Coord. Chem.* **1985**, *14*, 139–149.
(26) Buglyo, P.; Kiss, T.; Dyba, M.; Jezowska-Bojczuk, M.; Kozlowski, H.; Bouhsina, S. *Polyhedron* **1997**, *16*, 3447–3454.
(27) Sawada, K.; Kanda, T.; Naganuma, Y.; Suzuki, T. *J. Chem. Soc., Dalton Trans.* **1993**, 2557, 2562.

Table 1. Logarithms of the Stepwise Protonation Constants K_{ai} of Some Imino-*bis*(methylenephosphonic acids), R−N$^+$H(CH$_2$PO$_3$H$_2$)(CH$_2$PO$_3$H$^-$), LH$_4$

species, R	LH^{3-}, log K_{a1}	LH$_2^{2-}$, log K_{a2}	LH$_3^-$, log K_{a3}	LH$_4$, log K_{a4}	references
H^a	11.5 (0.1)	6.12 (0.1)	4.85 (0.01)	0.86	24 (LH), 25 (LH$_4$), 26
CH$_3$^{b}	12.1 (0.1)	6.04 (0.1)	4.90 (0.05)	1.3 (0.2)	25 (LH), 27
	11.75 (0.1)	5.95 (0.1)	4.79 (0.02)		28
C$_2$H$_5$^{c}	12.2 (0.1)	6.01 (0.1)	4.69 (0.04)	<2	28, 29 (LH$_4$)
HOCH$_2$CH$_2$^{d}	11.25 (0.02)	5.94 (0.02)	4.53 (0.04)	0.6 (0.2)	this work^e

^{a} Imino-*bis*(methylenephosphonic acid). ^{b} Methylimino-*bis*(methylenephosphonic acid). ^{c} Ethylimino-*bis*(methylenephosphonic acid). ^{d} Hydroxyethylimino-*bis*-(methylenephosphonic acid), HEIBPH, **1**. ^{e} These constants are determined in aqueous solutions containing 10 vol % D$_2$O; therefore, the values log K_i are 0.06−0.08 units larger than in solutions without D$_2$O.[38]

are shown in Table 1 and in Table S3 of the Supporting Information. Table S3 contains the direct obtainable cumulative protonation constants

$$\beta_i = [LH_i]/\{[L][H]^i\}$$

and also the individual chemical shifts δ_i, while the derivables from the β_i stepwise protonation constants

$$K_{ai} = \beta_i/\beta_{i-1} = [LH_i]/\{[LH_{i-1}][H]\}$$

are summarized in Table 1. We must take into account that the constants K_{a1} and K_{a2} are somewhat lowered due to formation of Na-containing species LNa^{3-} and LNaH^{2-}, which were not individually detectable. Strictly speaking, these constants are "apparent" constants.[36]

Literature values for imino-*bis*(methylenephosphonic acid) and for two other substituted compounds are included in Table 1. As expected, methyl and ethyl substituents cause a decrease in the acidity of the [R(PO$_3$)$_2$NH]$^{3-}$ species (see log K_{a1}), and the hydroxyethyl group increases it. However, decrease of the protonation constants K_{a1} and K_{a2} of HEIBPH, in comparison with those of imino-*bis*(methylenephosphonic acid), may be partially caused by the formation of weak complexes with Na$^+$ ions. The authors of the papers in refs 25−29 have used KNO$_3$ or KCl and KOH for titrations, whose K$^+$ ions show a minor tendency of complex formation with aminophosphonic acids.[36] The value of log K_{a4} is very small and cannot be determined accurately by titrations using a glass electrode. For an accurate determination of low pK values, Szakács and Hägele have proposed a special NMR methodology.[37]

A distribution diagram of the various protonated species of HEIBPH was calculated using the program HYSS[20] and

(28) Kurzak, B.; Kamecka, A.; Kurzak, K.; Jezierska, J.; Kafarski, P. *Polyhedron* **1998**, *17*, 4403–4413.
(29) Carter, R. P.; Carroll, R. L.; Irani, R. R. *Inorg. Chem.* **1967**, *6*, 939–942.
(30) Sawada, K.; Duan, W.; Ono, M.; Satoh, K. *J. Chem. Soc., Dalton Trans.* **2000**, *919*, 924.
(31) Sawada, K.; Ichikawa, T.; Uehara, K. *J. Chem. Soc., Dalton Trans.* **1996**, *3077*, 385.
(32) Popov, K.; Popow, A.; Rönkkömäki, H.; Lajunen, L. H. J.; Hannu-Kuure, M.; Vendilo, A.; Tsirul'nikova, N. *Inorg. Chim. Acta* **2003**, *344*, 1–6.
(33) Popov, K.; Rönkkömäki, H.; Lajunen, L. H. J. *Pure Appl. Chem.* **2001**, *73*, 1641–1677.
(34) Popov, K.; Rönkkömäki; Lajunen, L. H. J. *Pure Appl. Chem.* **2006**, *78*, 663–675.
(35) Lukeš, I.; Dominák, I. *Chem. Papers* **1988**, 311–317.
(36) Grossmann, G.; Burkov, K. A.; Hägele, G.; Myund, L. A.; Hermens, S.; Verwey, C.; Arat-ool, S. M. *Inorg. Chim. Acta* **2004**, *357*, 797–808.
(37) Szakács, Z.; Hägele, G. *Talanta* **2004**, *62*, 819–825.
(38) Dagnall, S. P.; Hague, D. N.; McAdam, M. E.; Moreton, A. D. *J. Chem. Soc., Faraday Trans 1* **1985**, *81*, 1483–1494.
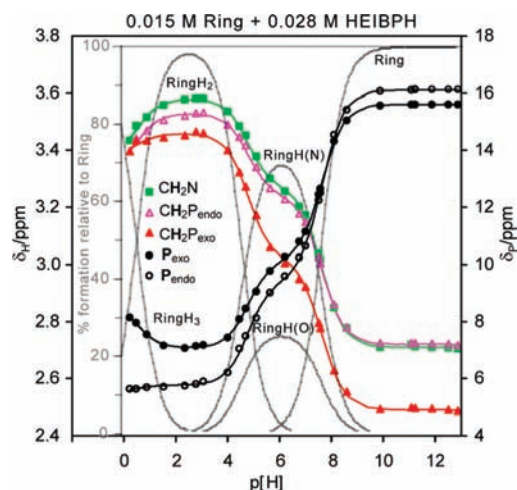
Figure 3. Single-sample ^{31}P and ^{1}H NMR titration curves δ versus p[H] of solutions of 0.015 M oxazaphosphorinane, **2**. The *solid lines* between the experimental values are drawn by joining calculated values, obtained using the refined equilibrium constants and the individual chemical shifts. *Gray lines* show the calculated species distribution of **2** (the charges of species are omitted).

is included in Figure 2. Virtually single species are present at pH 2.55 (98.0% LH$_3^-$), at pH 8.6 (99.6% LH^{3-}), and at pH > 13 (>98% L^{4-}).

The analysis of preliminary single-sample ^{31}P, ^{13}C, and ^{1}H titrations of 0.11 M HEIBPH solutions shows similar results (see Figure S3 and Table S4, Supporting Information). However, the precision of these results is not satisfactory, as only 12−14 solutions were included in the refinement. Further investigation of 0.11 M HEIBPH solutions was not pursued because abundant precipitate is formed at pH > 5 in the presence of 0.11 M CaCl$_2$.

NMR Acid−Base Titration of Solutions Containing Ring 2. Single-sample ^{31}P and ^{1}H titration curves of 2-hydroxy-2-oxo-4-phosphonemethyl-1,4,2-oxazaphosphorinane (**2**) were obtained by an investigation of solutions containing 0.015 M **2**, 0.028 M HEIBPH, and 0.007 M AMP. The titration results are shown in Figure 3. For data analysis by the HypNMR program, the signals due to the CH$_2$O protons were ignored because these data do not vary significantly over the whole p[H] range.

The results of refined calculations of protonation constants and individual chemical shifts are shown in Table 2 and Table S5 (Supporting Information). The assignment of the proton signals to CH$_2$ groups was ensured by a 2D ^{1}H/^{31}P correlation spectrum (see Figure S4, Supporting Information). The distribution diagram of the various species of ring **2** is also shown in Figure 3. Virtually single species are present

Table 2. Logarithms of Cumulative Protonation Constants β_i, Stepwise Protonation Constants K_{ai}, and Microscopic Protonation Constants $k_{i'}$ and $k_{i''}$ of 2-Hydroxy-2-oxo-4-phosphonemethyl-1,4,2-oxazaphosphorinane, **2**[a]

species, i	RingH^{2-}, 1	RingH$_2^-$, 2	RingH$_3$, 3
$\log \beta_i$	7.63 (0.01)	12.41 (0.02)	12.9 (0.1)
$\log K_{ai}$	7.63 (0.01)	4.78 (0.01)	0.5 (0.1)
$\log k_{i'}$	7.44 (0.01)	4.97 (0.01)	
$\log k_{i''}$	7.18 (0.01)	5.23 (0.01)	

[a] These constants are determined in aqueous solutions containing 10 vol % D$_2$O; therefore, the values $\log K_{ai}$ are 0.06−0.08 units larger than in solutions without D$_2$O.[38]

Scheme 2. Microscopic Protonation Equilibrium of Ring **2**
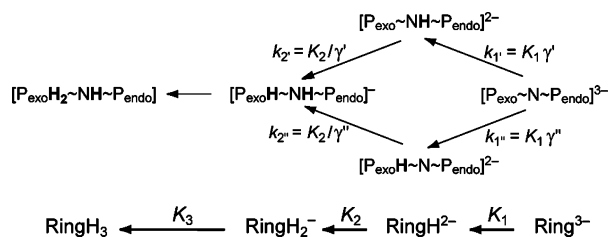
at pH 2.67 (98.6% RingH$_2^-$), at pH 6.22 (93.0% RingH^{2-}), and at pH >9.4 (>98% Ring^{3-}).

Ring **2** is a triacid; therefore, its first protonation constant K_{a1} is much smaller than the corresponding constant of the tetra-acid HEIBPH. A comparison of the curves δ_{Pexo} and δ_{Pendo} at pH < 3 (see Figure 3) points to the conclusion that the protonation state of the endo phosphonate groups remains nearly constant, but the exo phosphonate groups show increased protonation by decreasing pH. The crystal structure of **2** displays a "betain" structure with a proton-free endo phosphonate group and a proton at the nitrogen.[39]

In contrast to the titration curves of HEIBPH and other substituted imino-*bis*(methylenephosphonic acids), the increase of δ_P caused by the deprotonation of NH extends over a very broad range beginning at pH 3.5 and ending at ≈10. As shown in Figure 3, three macroscopic protonation states exist in this range, RingH$_2^-$, RingH^{2-}, and Ring^{3-}. Assuming two microscopic states without a proton at nitrogen, [P$_{exo}$∼N∼P$_{endo}$]$^{3-}$ and [P$_{exo}$**H**∼N∼P$_{endo}$]$^{2-}$, and two microscopic states with a proton attached to nitrogen, [P$_{exo}$∼**NH**∼P$_{endo}$]$^{2-}$ and [P$_{exo}$**H**∼**NH**∼P$_{endo}$]$^-$, we can describe the protonation equilibrium reactions as shown in Scheme 2.

The microscopic and the macroscopic constants are connected by the following equations:

$$K_1 = k_{1'} + k_{1''} \tag{3}$$

$$K_2^{-1} = k_{2'}^{-1} + k_{2''}^{-1} \tag{4}$$

$$K_1 \cdot K_2 = k_{1'} \cdot k_{2'} = k_{1''} \cdot k_{2''} \tag{5}$$

If we can estimate the splitting coefficients $\gamma' = k_{1'}/K_1$ or $\gamma'' = k_{1''}/K_1$ using a suitable property, all four microscopic equilibrium constants can be calculated.

In the case of HEIBPH, the upper method of protonation is favored ($\gamma' = 1$), and the process of formation of

(39) Makarenets, B. I.; Polynova, T. N.; Porai-Koshits, M. A.; Il'ichev, S. A. *J. Struct. Chem.* **1987**, *27*, 603–609.

Table 3. Differences of Individual Chemical Shifts $\Delta(j,k)^a$ (in ppm) and Splitting Coefficients γ'^b of 0.015 M Solution of 2-Hydroxy-2-oxo-4-phosphonemethyl-1,4,2-oxazaphosphorinane (**2**)

δ_i	$\Delta(0,1)$	$\Delta(1,2)$	$\Delta(0,2)$	γ'
$\delta_{Pi}(exo)$	−5.48	−3.08	−8.56	0.64
$\delta_{Pi}(endo)$	−6.68	−3.66	−10.34	0.65
$\delta_{Hi}(CH_2N)$	0.56	0.31	0.87	0.64
$\delta_{Hi}(CH_2P_{endo})$	0.52	0.29	0.81	0.64
$\delta_{Hi}(CH_2P_{exo})$	0.53	0.45	0.98	0.54

[a] $\Delta(j,k) = \delta_k - \delta_j$ with j,k indicating the number of acidic protons in a given microscopic state. [b] $\gamma' = \Delta(0,1)/\Delta(0,2)$.

[R(PO$_3$)$_2$NH]$^{3-}$ proceeds in a range of pH from 13 to 9. Strong changes of ^{31}P and ^{1}H chemical shifts accompany this process (see Figure 2). The next protonation on one of the phosphonate oxygens in the pH range 9−5 leads to marginal changes of chemical shifts. Only the ^{1}H chemical shift of the **CH$_2$P** group is an exception, increasing noticeably by this protonation.

In the case of ring **2**, we can use the individual chemical shift differences of the species Ring^{3-}, RingH^{2-}, and RingH$_2^-$, $\Delta(0,1) = \delta_1 - \delta_0$, $\Delta(1,2) = \delta_2 - \delta_1$, and $\Delta(0,2) = \delta_2 - \delta_0$, as a suitable property to estimate the splitting coefficients (see Table S5, Supporting Information, and Table 3):

$$y' = \Delta(0,1)/\Delta(0,2) \quad y'' = \Delta(1,2)/\Delta(0,2) \quad y' + y'' = 1 \tag{6}$$

Here, we assume the following relations for the individual chemical shifts of the microscopic states:

$$\delta(P_{exo}{\sim}NH{\sim}P_{endo})^{2-} - \delta(P_{exo}{\sim}N{\sim}P_{endo})^{3-} =$$
$$\delta(P_{exo}H{\sim}NH{\sim}P_{endo})^- - \delta(P_{exo}H{\sim}N{\sim}P_{endo})^{2-} \tag{7}$$

$$\delta(P_{exo}H{\sim}NH{\sim}P_{endo})^{2-} - \delta(P_{exo}{\sim}N{\sim}P_{endo})^{3-} =$$
$$\delta(P_{exo}H{\sim}NH{\sim}P_{endo})^- - \delta(P_{exo}{\sim}NH{\sim}P_{endo})^{2-} = 0 \tag{8}$$

The equal values of γ' in Table 3 show that the assumptions made are valid for these nuclei. For $\delta_{Hi}(CH_2P_{exo})$, another value of γ' was found because the equation (eq 8) is *not* valid. With $\gamma' = 0.64$, the microscopic equilibrium constants in Table 2 and the distribution of the species (P$_{exo}$∼NH∼P$_{endo}$)$^{2-}$ [RingH(N)] and (P$_{exo}$H∼N∼P$_{endo}$)$^{2-}$ [RingH(O)] in Figure 3 were calculated. The microscopic individual chemical shifts are included in Table S5 (Supporting Information). In this way, it was possible to determine the microscopic protonation constants k_{1i} and k_{2i} of **2** on the basis of a comparison of NMR titration curves of **1** and **2**.

Formation of Ca−HEIBPH Complexes. Single-sample ^{31}P and ^{1}H titration curves of 0.05 M HEIBPH + 0.05 M CaCl$_2$ + 0.26 M Na$^+$ are shown in Figure 4. In the data analysis, we did not include the ^{1}H titration curve of the **CH$_2$OH** protons, giving only small changes of the chemical shift over the whole pH range. As shown in Figure S5 (Supporting Information), the titration curves of series with and without Ca^{2+} coincide with pH = 3; therefore, the first Ca^{2+} species in acid solutions with pH > 3 is probably LCaH$_2$. Beginning the analysis of δ versus pH curves with pH = 2, we can omit the species LH$_4$ (see Figure 2).

At increased pH, we expect the formation of species LCaH$_2$, LCaH$^-$, LCa^{2-}, and LCa$_2$, besides LH$_3^-$, LH$_2^{2-}$,
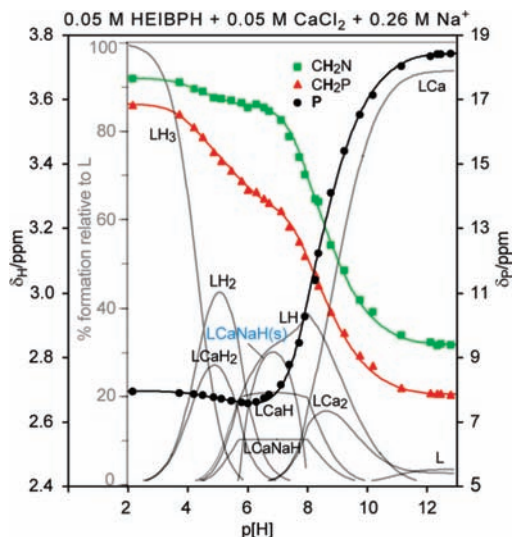
Figure 4. Single-sample ^{31}P and ^1H NMR titration curves δ versus p[H] of solution containing 0.05 M HEIBPH (**1**), 0.05 M CaCl$_2$, and 0.26 M Na$^+$. The *solid lines* between the experimental values are drawn by joining calculated values, obtained using the simulated equilibrium constants and the supposed individual chemical shifts. *Gray lines* show the calculated species distribution (charges of species are omitted).

LH^{3-}, and L^{4-}. In addition, we must take into consideration the formation of a precipitate LCaNaH in some of the samples (see Experimental Section, Materials). Therefore, the equilibrium state of the species LCaNaH must be characterized also by β(LCaNaH) and by the solubility product constant K_{sp}(LCaNaH). The cumulative equilibrium constants in the presence of metal ions

$$\beta(LCa_mNa_nH_p) = [LCa_mNa_nH_p]/\{[L][Ca]^m[Na]^n[H]^p\}$$

describe complex formation and protonation equilibrium. From these cumulative constants, the stepwise calcium complex formation constants

$$K_c(LCa_mNa_nH_p) = \beta(LCa_mNa_nH_p)/\beta(LCa_{m-1}Na_nH_p) =$$
$$[LCa_mNa_nH_p]/\{[LCa_{m-1}Na_nH_p][Ca]\}$$

and the stepwise protonation constants

$$K_a(LCa_mNa_nH_p) = \beta(LCa_mNa_nH_p)/\beta(LCa_mNa_nH_{p-1}) =$$
$$[LCa_mNa_nH_p]/\{[LCa_mNa_nH_{p-1}][H]\}$$

can be derived.

The equilibrium constants and chemical shifts of the Ca^{2+} species were changed step-by-step by manually adjusting the calculated δ versus [pH] curves to the experimental data points at the output viewer of the HypNMR program. The solubility product constant K_{sp}(LCaNaH) = −15.45 was chosen in such a way that a maximum amount of 30% of the total P is located in the solid phase. The speciation curves in Figure 4 are a result of such analysis.

Unfortunately, the analysis of the titration data leads to ambiguous solutions: two protonation constants give good fitting of the δ versus p[H] curves for opposite pairs of

(40) Matczak-Jon, E.; Kurzak, B.; Kamecka, A.; Sawka-Dobrowolska, W.; Kafarski, P. *J. Chem. Soc., Dalton Trans.* **1999**, *3627*, 3637.

Table 4. Logarithms of Stepwise Complex Formation Constants K_{ci}(Ca) and Protonation Constants K_{ai} of Species LCa$_m$Na$_n$H$_p$[a] in Some Imino-*bis*(methylenephosphonic acids), [R−N$^+$H(CH$_2$PO$_3$H$_2$)-(CH$_2$PO$_3$H$^-$)]

| equilibrium[a] | L = [R−N(CH$_2$PO$_3$)$_2$]$^{4-}$ | | | |
	R = H[b]	H[c]	CH$_3$[c]	CH$_2$CH$_3$[c]	CH$_2$CH$_2$OH[d]
L + Ca	3.84	3.11	4.11	3.71	4.74
LH + Ca	2.43	1.82	2.28	2.39	1.60
LH$_2$ + Ca	1.71	0.67	1.43	1.67	1.29
LCa + Ca					1.78
LCaH + Na					0.31
LCa + H	9.38	9.31	9.92	10.88	8.11
LCaH + H	5.36	4.67	5.10	5.29	5.63
LCa + OH		1.95	0.93		

[a] The charges are omitted. [b] Ref 25. [c] Ref 40. [d] This work. These constants are determined in solutions of 0.05 M HEIBPH (**1**) + 0.05 M CaCl$_2$ + 0.26 M Na$^+$ containing 10 vol % D$_2$O.

β(LCaH) and β(LCaNaH) in the range of values 13.0−12.13 for log β(LCaH) and 12.7−13.56 for log β(LCaNaH). Since the Na$^+$ complexes are much weaker than the Ca^{2+} complexes, we prefer the pair of constants log β(LCaH) = 12.85 ± 0.2 and log β(LCaNaH) = 13.16 ± 0.2.

A compilation of chosen cumulative complex formation constants used for the presentation of the speciation diagram in Figure 4 is shown in Table S6 (Supporting Information), which also contains the individual chemical shifts of the Ca^{2+} species. Logarithms of the stepwise complex formation constants K_{ci}(M) and protonation constants K_{ai} of Ca^{2+} containing species are summarized in Table 4. Some results obtained at a few substituted imino-*bis*(methylenephospho-nates) described in the literature[25,40] were included in Table 4. Although, most constants lie in a comparable range, our results differ from the literature data in the experimental conditions used. The high concentration of Na$^+$ ions in the alkaline stock solution (τ = 5.2) leads to formation of the complex LCaNaH and to its partial precipitation. In addition, we must include the formation of LCa$_2$ as well to fit the calculated titration curves into experimental curves in the pH region 8−10. This species was not considered in the literature. On the other hand, LCaOH[40] was not considered in our investigation.

Very broad NMR lines were obtained in the range in which species coexist, having large differences in chemical shifts. Specifically, the ^{31}P line of the sample at pH = 8.78 and δ = 14.1 shows $\nu_{1/2}$ = 810 Hz. At this point, five species coexist, leading to a sufficiently low exchange of Ca^{2+} between the low chemical shift species LH (30.2%), LCaH (8.7%), and LCaNaH(4.4%), on the one hand, and the high chemical shift species LCa (40.8%) and LCa$_2$ (15.7%), on the other hand. In the same range, the ^1H lines are less broadened; the CH$_2$N signals have a maximum line broadening of 30 Hz and the CH$_2$P signal of 20 Hz.

The question of whether the N of HEIBPH is involved in Ca^{2+} binding can be addressed as follows: All species possessing one or more acidic protons contain a quaternary N atom and cannot bind Ca^{2+} or other metal ions. Due to the affinity of the Ca^{2+} ions for N, its deprotonation occurs at lower pH, and the formation of species LCa, LCa$_2$, and LCaNa is observed. Comparison of the ^1H titration curves of HEIBPH with and without Ca^{2+} in Figure S5 (Supporting

Scheme 3. Conformational States of **2** Caused by Ring Inversion and by Change of Configuration

$$^3J_{HH}: \quad p_{I_{(R)}} + p_{II_{(S)}} = p_c = p_{II_{(R)}} + p_{I_{(S)}} = 0.5$$
$$^3J_{PC}: \quad p_{I_{(R)}} + p_{I_{(S)}} = p_I \quad p_{II_{(R)}} + p_{II_{(S)}} = p_{II} \quad p_I + p_{II} = 1$$

$$p_{I_{chair}} = [^3J(P_{endo}\text{-}C7) - J_g] / (J_t - J_g) \qquad p_{II_{chair}} = 1 - p_{I_{chair}}$$

$$p_{I_{rot}} = [^3J(P_{exo}\text{-}C3) - J_g] / (J_t - J_g)$$
$$p_{II_{rot}} = [^3J(P_{exo}\text{-}C5) - J_g] / (J_t - J_g) \qquad p_{III_{rot}} = 1 - p_{I_{rot}} - p_{II_{rot}}$$

Figure 5. Conformational states in ring **2** around the bonds N−C3 and N−C7.

Information) shows a noticeable influencing of the CH_2OH chemical shift in the presence of Ca^{2+} at high pH values. This fact implicates the possibility of Ca^{2+} binding by the hydroxyl group. Coordination of Na^+ ions by N *and* the hydroxyl group has been demonstrated in the crystal structure of LNa_4.[9]

Conformation States in 1 and 2. By using the three-bond coupling constants, we can obtain useful information on the conformation states of the investigated compounds, ring inversion, equatorial or axial arrangements of the CH_2P_{exo} group, and rotation states around the N−C bonds in **2** and several rotation conformations in **1**. Relevant couplings are the $^3J_{HH}$ and, particularly, the coupling constants $^3J_{PC}$ obtained from high-resolution ^{13}C spectra (see Tables S7 and S8, Supporting Information). A $^1H-{}^{13}C$ 2D correlation spectrum allows unambiguous assignment of the ^{13}C signals in **2** (see Figure S6, Supporting Information).

The ^1H spectra of the $HO-CH_2-CH_2N$ fragment of **1** and the $O-CH_2-CH_2N$ fragment of **2** provide some initial information. All spectra of **1** show for this group a typical AA′BB′ and those of **2** an AA′BB′X spin system (see Figure S7, Supporting Information). The low-field BB′ signal from the OCH_2 group of **2** shows a doublet splitting caused by coupling with the P_{endo} nucleus as X spin, and the AA′ signal of both compounds is slightly broadened by coupling with nuclei through four bonds.

The crystal structure of acid **2** shows a chair form of the ring and an equatorial CH_2P_{exo} group.[39] Two different chair conformations I_{chair} and II_{chair} result from fast ring inversion in solution at room temperature. The probabilities p_I and p_{II} cannot be equal if I_{chair} has an *equatorial* and II_{chair} an *axial* CH_2P_{exo} group. In such a case, the protons H and H′ of each CH_2 group of the fragment $O-CH_2-CH_2N$ have different mean chemical shifts, and the considered fragment must give an ABCD spin system in the ^1H NMR spectrum of **2**.

As shown in Scheme 3, only a change in the configuration at the N atom can explain the occurrence of AA′BB′ spin systems, which are very similar to the AA′XX′ type. The change of configuration is possible because the proton at the N is exchangeable. Another compound with a similar ring, 3-ethyl-2-hydroxy-2-oxo-oxazaphosphorinane, has a chiral carbon center, which prohibits a change of configuration. Therefore, this compound shows an ABCD spin system for the fragment $O-CH_2-CH_2N$.[41a]

The analysis of the AA′BB′X spin system by spectrum simulation of **2** gives the mean coupling constants $^3J(AB)$ and $^3J(AB')$, which are weight mean values of *trans* and *gauche* coupling constants J_t and J_g characterizing the

Table 5. Probabilities p_i of Inversional and Rotational States Based on Experimental Coupling Constants ^3J and Using Coupling Constants J_t and J_g (in Hz) for Solutions of Oxazaphosphorinane **2**

conformation	pH	$^3J_{HCCH}$	$^3J_{HCCH'}$	J_t	J_g	$p_c{}^a$	$p_c{}^a$	
ring inversion	<6	6.85	2.6	11.1	2.6	0.50	0.50	
	>10	6.25	3.1	9.4	3.1	0.50	0.50	
		$^3J_{P_{endo}C3NC7}$	$^3J_{P_{endo}\cdots C5}{}^b$			$p_{I_{chair}}{}^c$	$p_{II_{chair}}{}^c$	
ring inversion	0.9	7.8	4.4	20^d	2.2	0.31	0.69	
	3.34	7.9	4.2	20^d	2.1	0.32	0.68	
	5.60	10.9	3.8	19.5^d	1.9	0.51	0.49	
	12.8	17.9	3.2	17.9	1.6	≈1.0	≈0.0	
		$^3J_{P_{exo}C7NC3}$	$^3J_{P_{exo}C7NC5}$			$p_{I_{rot}}$	$p_{II_{rot}}$	$p_{III_{rot}}$
rotation $P_{exo}C7-NC3/5$	0.9	3.8	5.8	20	2.2	0.09	0.20	0.71
	3.34	3.9	5.8	20	2.1	0.10	0.21	0.69
	5.60	5.1	5.9	19.5	1.9	0.18	0.23	0.59
	12.8	9.3	8.2	17.9	1.6	0.47	0.40	0.13

$^a p_c = p_{I_{(R)}} + p_{II_{(S)}} = p_{II_{(R)}} + p_{I_{(S)}} = 0.5$ (see Scheme 3). ^{b} Two coupling ways exist: $P_{endo}-C3-N-C5$ and $P_{endo}-O-C6-C5$. $^c p_{I_{chair}} = p_{I_{(R)}} + p_{I_{(S)}}$ and $p_{II_{chair}} = p_{II_{(R)}} + p_{II_{(S)}}$ (see Scheme 3). ^{d} Assumed values.

Figure 6. Roughly estimated probabilities of proposed oxazaphosphorinane conformers **2**. All molecules also occur in the form of their mirror images.

different conformational states taking into account a fast ring inversion and a change of configuration at N.
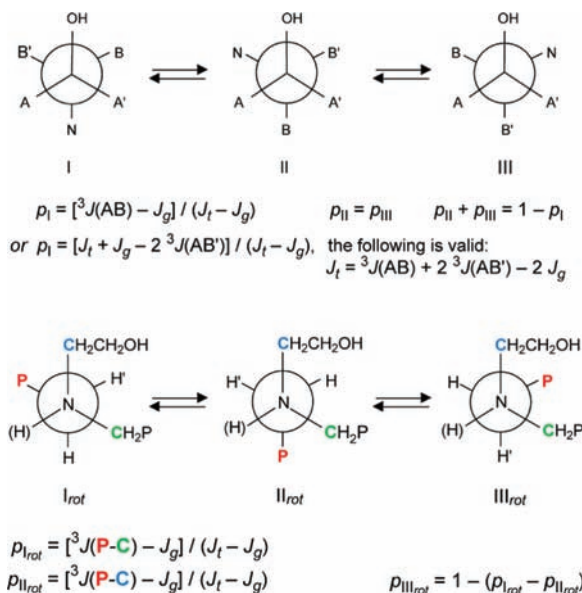
$$^3J(AB') = (J_g + J_g)/2 = J_g \qquad (9)$$

$$^3J(AB) = (J_t + J_g)/2 \quad 2\,^3J(AB) - \,^3J(AB') = J_t \quad (10)$$

As shown in Table 5, the three-bond H−H coupling constants J_t and J_g calculated with eqs 9 and 10 were found in the expected range.[42] Possible conformational states generated by ring inversion and by rotation around the N−C7 bond in **2** are represented in Figure 5. The three-bond P−C−N−C coupling constants are important values for investigation of the conformational states in **1** and **2** because they allow for conclusions about their probabilities p_i. Assuming only chair conformations of the ring structure, we have obtained reasonable results of J_t and J_g and of the probabilities of inversional $p_{i_{chair}}$ and rotational states $p_{i_{rot}}$ (see Table 5).

The dihedral angle $P_{endo} \cdots C5$ remains in the *gauche* position by inversion of the ring. At the same time, there exist two coupling pathways, P_{endo}−C3−N−C5 and P_{endo}−O−C6−C5, allowing, as a first approximation, to assume that $^3J_{P_{endo} \cdots C5} \approx 2\,J_g$. The equilibrium between *equatorial* and *axial* positions of the CH_2P_{exo} group is indicated by $^3J_{P_{endo}C3NC7}$, giving J_t in the case of only *equatorial* conformation and J_g in that of only *axial*. If all acid protons are removed at pH > 10, a maximum value of $^3J_{P_{endo}C3NC7} \approx 18$ Hz is obtained.

This value is similar to J_t in phosphonates of the type P−C−C−C;[43] therefore, we assume that, at these conditions, the CH_2P_{exo} group exists only in the *equatorial* position of

(41) (a) Troev, K.; Hägele, G.; Kreidler, K.; Olschner, R.; Verwey, C.; Roundhill, D. M. *Phosphorus, Sulfur, Silicon* **1999**, *148*, 161–176. (b) Troev, K.; Cremer, S.; Hägele, G. *Heteroatom Chem.* **1999**, *10*, 627–631.
(42) (a) Pachler, K. G. R. *Spectrochim. Acta* **1964**, *20*, 681–687. (b) Haasnoot, C. A. G.; de Leeuw, F. A. A. M.; Altona, C. *Tetrahedron* **1980**, *36*, 2783–2792.
(43) (a) Thiem, J.; Meyer, B. *Org. Magn. Reson.* **1978**, *11*, 50–51. (b) Adiwidjaja, G.; Meyer, B.; Thiem, J. *Z. Naturforsch.* **1979**, *34b*, 1547–1551. (c) Quin, L. D.; Gallagher, M. J.; Cunkle, G. T.; Chesnut, D. B. *J. Am. Chem. Soc.* **1980**, *102*, 3136–3143. (d) Grossmann, G.; Lang, R.; Ohms, G.; Scheller, D. *Magn. Reson. Chem.* **1990**, *28*, 500–504.

Figure 7. Conformational states in **1** around the C−C and the N−C(P) bonds.

conformation I_{chair}. The three rotational conformation states lead to an equilibrium of three conformers in a sufficient basic medium: 1b (I_{chair}; I_{rot}), 2b (I_{chair}; II_{rot}), and the minor conformer 3b (I_{chair}; III_{rot}). Because of the limited point resolution of the ^{13}C spectra and the uncertainties in the *trans* and *gauche* coupling constants, we approximated the listed values for probabilities p_i of conformers to one tenth in Figure 6. Note that the different conformers form a fast dynamic system with transitions of one into the other by jumps.

When at least one proton is added to the phosphonate group $CH_2P_{exo}O_3$, the preferred chair conformation II_{chair} has this group in the *axial* position. This conformation is accompanied by the rotation state III_{rot} having nearly the same probability as the inversion state II_{chair} in an acidic medium: $p_{II_{chair}} \approx p_{III_{rot}} = 0.7$. Such conformers 1a ($II_{chair}$; III_{rot}) allow the formation of an energetically favorable intramolecular hydrogen bond between the two phosphonate groups. The steric hindrance of the *axial* CH_2P_{exo} group is probably decreased by increasing of the angle N−C−P and by some changes of relevant dihedral angles. In an acidic

Table 6. Probabilities p_i of Rotational States Based on Experimental Coupling Constants ^3J and using trans and gauche Coupling Constants J_t and J_g (in Hz) for Solutions of HEIBPH (**1**)

conformation	pH	$^3J_{HCCH}$	$^3J_{HCCH'}$	J_t	J_g	p_I	p_{II}	p_{III}
rotation	<10	6.5	4.0	9.3	2.6[a]	0.58	0.21	0.21
NCH$_2$−CH$_2$OH	>13	5.95	4.55	8.85	3.1[a]	0.50	0.25	0.25

		$^3J_{PCNC(P)}$	$^3J_{PCNC(C)}$			$p_{I_{rot}}$	$p_{II_{rot}}$	$p_{III_{rot}}$
rotation	0.7	4.2	3.8	20[a]	2.2	0.11	0.09	0.80
PCH$_2$−NCH$_2$	3.34	4.2	3.8	20[a]	2.1	0.12	0.09	0.79
	5.27	3.7	3.7	19.5[a]	1.9	0.10	0.10	0.80
	10.29	4.4	3.7	19.0[a]	1.8	0.15	0.11	0.74
	10.55	5.3	3.7	19.0[a]	1.7	0.21	0.12	0.67
	12.8	9.0	6.1	17.9	1.6	0.45	0.28	0.27
	13.3	9.4	6.3	17.9	1.6	0.48	0.29	0.23

[a] Assumed value.

medium, the chair conformation I_{chair} with an *equatorial* position of the CH$_2$P$_{exo}$ group has nearly the same probability as the sum of the two rotation conformations $p_{I_{chair}} \approx p_{II_{rot}} + p_{I_{rot}} = 0.3$. Therefore, we can expect the existence of conformers 2a (I_{chair}; II_{rot}) and 3a (I_{chair}; I_{rot}). It is notable that conformer 2a was found in the crystal of **2**.[39] A possible picture of the conformers of **2** is shown in Figure 6.

For **1**, the analysis of AA′BB′ spectra shows a slightly preferred *trans* conformation NCH$_2$−CH$_2$OH of $p_t \approx 0.5$ over the two equivalent gauche conformations in the whole pH range. Possible conformational states generated by rotation around the C−C bond and the two N−C(P) bonds in **1** are represented in Figure 7. Results of the analysis are summarized in Table 6.

In alkaline solutions, we can assume two types of conformers in **1** (see Figure 8): each of these has around the N−C(P2) bond the conformational state I_{rot} and around the N−C(P1), bond state II_{rot} or III_{rot}. The first preferred type is combined with a conformation state II around the C−C bond: 1b ($II_{rot,1}$; $II_{rot,2}$; II). In the crystal structure of Na$_4$HEIBPH·10H$_2$O,[9] this combination of conformational states and, in addition, almost a *trans* conformation was found for the CC−NC(P2) sequence. The second type includes conformer 2b ($III_{rot,1}$; $I_{rot,2}$; I). The conformational states of the CC−NC(P) sequences remain uncertain.

Profound changes in the conformational states occur if the first proton is bonded to N. These states persist in acidic solutions. We assume the occurrence of three types of conformers: 1a ($III_{rot,1}$; $III_{rot,2}$; I), 2a ($I_{rot,1}$; $III_{rot,2}$; III), and 3a ($II_{rot,1}$; $III_{rot,2}$; III). All of these conformers allow the

formation of an intramolecular hydrogen bond between two phosphonate groups (perhaps by involvement of a water molecule) or between the hydroxyl proton of the CH$_2$OH group and the O of PO$_3$ groups.

Conclusions

The open form of HEIBPH (**1**) converts to the self-condensation product **2** (Scheme 1) in acidic solutions, as evidenced by multinuclear NMR spectroscopy. For example, after a standing time of 180 days at 22 °C of 0.05 M solutions of **1**, the formation of nearly 6, 18, and 55% of **2** is obtained for solutions containing 0.05, 0.15, and 0.55 M HCl, respectively.

When NMR titration curves are used without and with Ca^{2+}, the protonation and complex formation constants are obtained, allowing calculation of distribution diagrams for the various species of **1**. Additionally, comparison of the ^{1}H titration curves of **1** shows a noticeable influencing of the CH$_2$OH chemical shift in the presence of Ca^{2+} at high pH values. This fact implicates the hydroxyl group in Ca^{2+} binding. The species without acid protons on the N do have the ability to bind Ca^{2+}. These are LCa, LCa$_2$, and LCaNa. An unexpected result was the precipitation of LCaNaH in excess of Na$^+$.

Knowledge of the solution behavior of polyphosphonates is essential for their successful use as scale inhibitors. As shown in this work, pH and the presence of metal ions strongly influence the protonation degree and metal binding (Ca^{2+} in our case, an abundant ion in process streams). For HEIBPH in particular, its use is not recommended in acidic process water streams, as it forms the self-condensation ring compound. It has been shown that, although HEIBPH is an effective CaCO$_3$ inhibitor, the ring byproduct is totally inactive.[44] Also, HEIBPH is especially calcium-tolerant.[45] According to preliminary studies,[44] as little as 12 ppm of AMP results in the formation of Ca−AMP precipitates when added to a solution of 1000 ppm Ca^{2+} at pH 9. This is in direct contrast with calcium tolerance results obtained with HEIBPH. A Ca−HEIBPH complex starts precipitating at concentrations of 4400 ppm of Ca^{2+} and ~29 000 ppm of HEIBPH at pH > 5. Detailed calcium tolerance studies will appear in due course. It is well-known that metal-inhibitor precipitates pose a serious problem in
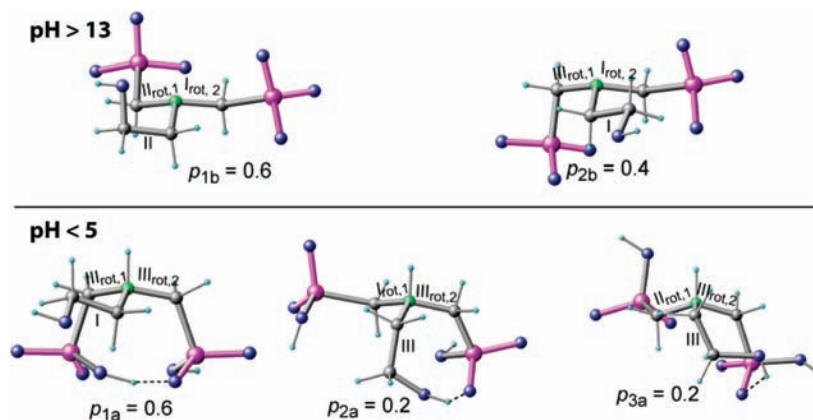
Figure 8. Roughly estimated probabilities p_i of proposed HEIBPH conformers **1**. All molecules also occur in the form of their mirror images.

process streams.[46] Delineation of metal−inhibitor interactions in aqueous solutions, as well as in the solid state, may reveal information that may prove useful in the proper application of scale inhibitors.

Supporting Information Available: A total of seven figures and eight tables show original NMR spectra (1D and 2D), titration curves, protonation constants, chemical shifts, and information on precipitate analyses. This material is available free of charge via the Internet at http://pubs.acs.org.

IC802400R

(44) Demadis, K. D.; Barouda, E. Unpublished results.

(45) "Tolerance" is defined in this context as the resistance of a phosphonate (or a chemical additive in general) to precipitation as its metal salt (see ref 12f). The most common metal ions present in process streams are Ca^{2+}, Mg^{2+}, Sr^{2+}, and Ba^{2+}, with Ca^{2+} being the most common. This is why the term "calcium tolerance" is frequently used.

(46) (a) Masler, W. F.; Amjad, Z. *Corrosion/88*, Paper No. 11 (National Association of Corrosion Engineers, Houston, TX, 1988. (b) Deluchat, V.; Bollinger, J.-C.; Serpaud, B.; Caullet, C. *Talanta* **1997**, *44*, 897. (c) Oddo, J. E.; Tomson, M. B. *Appl. Geochem.* **1990**, *5*, 527. (d) Demadis, K. D.; Yang, B.; Young, P. R.; Kouznetsov, D. L.; Kelley, D. G. In *Advances in Crystal Growth Inhibition Technologies*; Amjad, Z., Ed.; Plenum Publishing Corporation: New York, 2000; Chapter 16, p 215.